

# CD-insensitive PMD monitoring based on RF power measurement

Jing Yang,<sup>1</sup> Changyuan Yu,<sup>1,2,\*</sup> Linghao Cheng,<sup>3</sup> Zhaohui Li,<sup>3</sup> Chao Lu,<sup>4</sup>  
Alan Pak Tao Lau,<sup>4</sup> Hwa-yaw Tam,<sup>4</sup> and P. K. A. Wai<sup>4</sup>

<sup>1</sup>Department of Electrical & Computer Engineering, National University of Singapore 117576, Singapore

<sup>2</sup>Modulation and Coding Department, A\*STAR Institute for Infocomm Research (I2R), 138632, Singapore

<sup>3</sup>Institute of Photonics Technology, Jinan University, Guangzhou, 510632, China

<sup>4</sup>Photonic Research Centre, The Hong Kong Polytechnic University, SAR Hong Kong

\* eleyc@nus.edu.sg

**Abstract:** We propose and experimentally demonstrate a chromatic dispersion (CD)-insensitive first-order polarization mode dispersion (PMD) monitoring method based on radio-frequency (RF) power measurement. In high-speed (>10-GSym/s) transmission systems, a narrowband fiber Bragg grating (FBG) notch filter filters out the optical components at 10GHz away from the carrier. After square-law detection, the 10-GHz RF tone changes with PMD and is insensitive to CD, which can be used as a PMD monitoring signal. Compared with the monitoring techniques utilizing clock tone, the PMD measurement range is increased from 26.3-ps to 50-ps while the requirement of the bandwidth of photodetector is reduced from 19GHz to 10GHz in 19-Gsym/s systems. It is experimentally shown that this technique is efficient on CD-insensitive first-order PMD monitoring for 38-Gbit/s DQPSK and 57-Gbit/s D8PSK systems.

©2011 Optical Society of America

**OCIS codes:** (060.2330) Fiber optics communication; (060.2360) Fiber optics links and subsystems; (260.2030) Dispersion.

---

## References and links

1. H. Sunnerud, B.-E. Olsson, and P. A. Andrekson, "Measurement of polarization mode dispersion accumulation along installed optical fibers," *IEEE Photon. Technol. Lett.* **11**(7), 860–862 (1999).
2. C. D. Poole, R. W. Tkach, A. R. Chraplyvy, and D. A. Fishman, "Fading in lightwave systems due to polarization-mode dispersion," *IEEE Photon. Technol. Lett.* **3**(1), 68–70 (1991).
3. B. W. Hakki, "Polarization mode dispersion compensation by phase diversity detection," *IEEE Photon. Technol. Lett.* **9**(1), 121–123 (1997).
4. F. Roy, C. Francia, F. Bruyere, and D. Penninckx, "A simple dynamic polarization mode dispersion compensator," *Opt. Fiber Commun./Nat. Fiber Opt. Eng. Conf.(OFC/NFOEC)*, 275–278, vol. 1, 1999.
5. N. Kikuchi, "Analysis of signal degree of polarization degradation used as control signal for optical polarization mode dispersion compensation," *J. Lightwave Technol.* **19**(4), 480–486 (2001).
6. B. L. Heffner, "Automated Measurement of Polarization Mode Dispersion Using Jones Matrix Eigenanalysis," *IEEE Photon. Technol. Lett.* **4**(9), 1066–1069 (1992).
7. R. M. Jopson, L. E. Nelson, and H. Kogelnik, "Measurement of Second-Order Polarization-Mode Dispersion Vectors in Optical Fibers," *IEEE Photon. Technol. Lett.* **11**(9), 1153–1155 (1999).
8. M. Boroditsky, M. Brodsky, N. J. Frigo, P. Magill, and J. Evankow, "Viewing polarization 'strings' on working channels: High-resolution heterodyne polarimetry," *European Conference on Optical Communications Proceedings (ECOC)*, pp. 318–319, 2004.
9. M. Boroditsky, M. Brodsky, N. J. Frigo, P. Magill, and J. Evankow, "Estimation of eye penalty and PMD from frequency-resolved in-situ SOP measurements," *Proc. 17th Annual Meeting of the IEEE Lasers and Electro-Optics Society*, pp.88- 89, 2004.
10. S. Wang, A. Weiner, M. Boroditsky, and M. Brodsky, "Monitoring PMD-induced penalty and other system performance metrics via a high-speed spectral polarimeter," *IEEE Photon. Technol. Lett.* **18**(16), 1753–1755 (2006).
11. K. E. Cornick, K. Hinton, S. D. Dods, and P. M. Farrell, "Comparison of Methods for Monitoring PMD-Induced Penalty," *Opt. Fiber Commun./Nat. Fiber Opt. Eng. Conf.(OFC/NFOEC)*, pp. 783–785, 2007.
12. F. Buchali, W. Baumert, H. Bulow, and J. Poirrier, "A 40 Gb/s eye monitor and its application to adaptive PMD compensation," *Opt. Fiber Commun./Nat. Fiber Opt. Eng. Conf.(OFC/NFOEC)*, 202–203, vol. 1, 2002.
13. T. B. Anderson, A. Kowalczyk, K. Clarke, S. D. Dods, D. Hewitt, and J. C. Li, "Multi impairment monitoring for optical networks," *J. Lightwave Technol.* **27**(16), 3729–3736 (2009).

14. G. Ishikawa and H. Ooi, "Polarization-mode dispersion sensitivity and monitoring in 40-Gbits OTDM and 10-Gbits NRZ transmission experiments," *Opt. Fiber. Commun. (OFC)*, 117–119, 1998.
  15. Z. Pan, Q. Yu, Y. Xie, S. A. Havstad, A. E. Willner, D. S. Starodubov, and J. Feinberg, "Chromatic dispersion monitoring and automated compensation for NRZ and RZ data using clock regeneration and fading without adding signaling," *Opt. Fiber Commun. (OFC)*, p. WH5–1–3, vol.3, 2001.
  16. S. M. R. M. Nezam, Y. W. Song, C. Yu, J. E. McGeehan, A. B. Sahin, and A. E. Willner, "First-order PMD monitoring for NRZ data using RF clock regeneration techniques," *J. Lightwave Technol.* **22**(4), 1086–1093 (2004).
  17. C. Yu, Y. Wang, T. Luo, Z. Pan, S. M. R. Motaghian Nezam, A. B. Sahin, and A. E. Willner, "Chromatic-dispersion-insensitive PMD monitoring for NRZ data based on clock power measurement using a narrowband FBG notch filter," *European Conference on Optical Communications Proceedings (ECOC)*, Tu4.2.3, 1–2, 2003.
  18. K. J. Park, C. J. Youn, J. H. Lee, and Y. C. Chung, "Performance comparisons of chromatic dispersion-monitoring techniques using pilot tones," *IEEE Photon. Technol. Lett.* **15**(6), 873–875 (2003).
- 

## 1. Introduction

PMD is one of the major factors which limit the transmission length of high-speed wavelength-division-multiplexing (WDM) systems. PMD accumulates in the fiber link [1] and many in-line components. It is time varying, temperature dependent and may change with the network reconfigurations [2]. Besides, the instantaneous first-order PMD, also known as differential group delay (DGD), follows a Maxwellian probability distribution, which induces the possibility of network outage. Therefore, real-time PMD monitoring is essential to ensure robust transmission through long fiber links. Several methods have been proposed on PMD monitoring and compensation. One method was proposed measuring the difference between two orthogonal principal states of polarization (PSPs) [3]. However, polarization tracking is required in the system. Another method was reported to measure the DGD by monitoring the degree-of-polarization (DOP) of received signal [4, 5]. This method is dependent on the pulse width of the signal and the DGD monitoring range is small for short pulses. Besides, it is also dependent on modulation formats. The PMD parameter of a fiber can be measured by Jones Matrix Eigen analysis [6] and Poincare Sphere analysis [7]. These methods require the PSPs information of both ends of fiber link, which is not practical in long-haul transmission systems. State of Polarization (SOP) string length has been shown related to PMD-induced power penalty [8–11], and it is robust to other impairments [11], such as CD, ASE and PDL. However, Polarimeter, which is expensive for real system, is required to obtain string length. Eye diagrams and delay-tap plots reveal the effect of PMD [12, 13], while it is still challenging to measure the value of PMD in the presence of other impairments. RF tone power can be used to monitor PMD [14], though it is also affected by chromatic dispersion (CD) [15]. CD-insensitive PMD monitoring techniques were proposed in [16, 17], where clock tone was used as the monitoring signal. The measurement range is limited, and the required bandwidth of photodetector (PD) is larger.

In this paper, a simple and cost effective CD-insensitive first-order PMD monitoring technique is proposed utilizing narrowband fiber Bragg grating (FBG) notch filter placed at 10-GHz away from the optical carrier in 57-Gbit/s and 38-Gbit/s transmission systems. The 10-GHz RF power, which changes as a function of PMD, was used as monitoring signal. This method has following advantages: 1) insensitive to chromatic dispersion; 2) wide measurement range; 3) low photoreceiver bandwidth requirement 4) no modification of the transmitter. It is experimentally shown that the proposed method is efficient for CD-insensitive first-order PMD measurement in differential 8-level phase-shift keying (D8PSK) and differential quadrature phase-shift keying (DQPSK) systems. The effects of optical signal-to-noise ratio (OSNR) and frequency detuning of FBG filter are shown in the simulation.

## 2. Operation principle

Optical signal propagating in optical transmission links is split into two orthogonal PSPs and each component travels along the fiber at different speeds due to the effect of DGD. Thus the two components are out-of-phase and the corresponding RF power is reduced through destructive interference. On the other hand, CD induces phase difference between the two

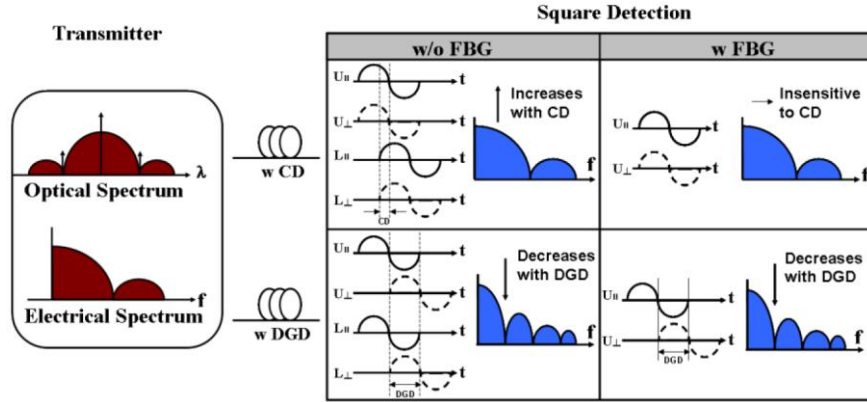


Fig. 1. Principle of PMD and CD effects on the RF power of NRZ signal.  $U_{11}$  ( $L_{11}$ ): signal of one PSP in upper (lower) sideband;  $U_{\perp}$  ( $L_{\perp}$ ): signal of the other PSP in upper (lower) sideband.

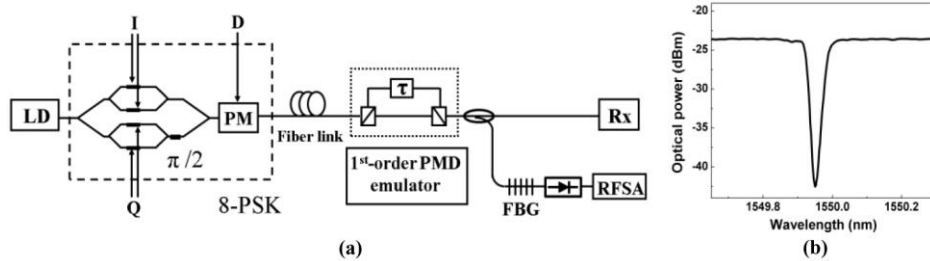


Fig. 2. (a) System setup of PMD monitoring utilizing FBG notch filter in an 8-PSK system; (b) measured optical transmission spectrum of FBG notch filter. LD: laser diode; PM: phase modulator.

sidebands and the RF power of the beating component is also affected by CD. Figure 1. shows the principle of PMD and CD effects on RF power of NRZ signal. In the absence of filter, both CD and PMD affect the RF power. If one sideband is filtered out, RF power changes with PMD and is insensitive to CD. The detected RF power of double sideband (DSB) can be expressed as [18]

$$P_{DSB} = P_0 \left[ 1 - 4\gamma(1-\gamma)\sin^2(\pi f_{RF} \Delta\tau) \right] (1 + \alpha^2) \times \cos^2 \left( \pi D \lambda^2 f_{RF}^2 / c + \arctan \alpha \right), \quad (1)$$

where  $P_0$  is RF power without CD and PMD effects;  $\gamma$  is the power splitting ratio between the two PSPs;  $\Delta\tau$  is the DGD of the link;  $\lambda$  is the carrier wavelength;  $f_{RF}$  is the RF frequency;  $c$  is the speed of light;  $\alpha$  is chirp parameter;  $\gamma$  and  $\Delta\tau$  are PMD induced parameters, and  $D$  is the collective dispersion parameter of fiber link and optical components. From (1), it is observed that both CD and PMD change the RF tone power in DSB signal and it is difficult to distinguish CD and PMD through RF power fading. If one of the sidebands is filtered out, the RF component power is insensitive to CD and only varies as a function of PMD [16]. The detected RF power of single sideband (SSB) is given by [16]

$$P_{SSB} = P_0 \left[ 1 - 4\gamma(1-\gamma)\sin^2(\pi f_{RF} \Delta\tau) \right] (1 + \alpha^2) \times |H(f_{RF})|^2 / 2, \quad (2)$$

where  $H$  is the electrical field transfer function of the optical filter. The division by 2 is due to the removal of one of sidebands. By using the detected RF power of SSB signal the effects of CD can be removed and DGD measurement can be achieved. It is also noted that the RF power of SSB signal changes periodically and the period is related to the RF frequency. From (2), the DGD measurement range is inversely proportional to RF frequency. Thus, DGD measurement range can be improved by using a low frequency RF tone as monitoring signal.

We propose a technique for CD-insensitive first-order PMD monitoring using a narrow

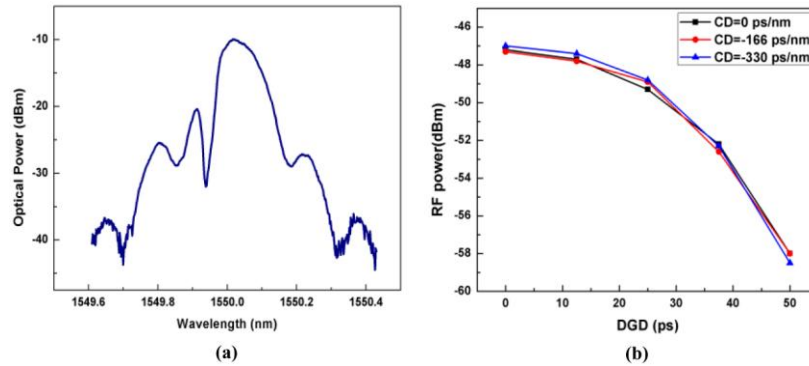


Fig. 3. (a) Optical spectrum of a 57-Gbit/s D8PSK signal filtered by an FBG notch filter placed at 10GHz away from the carrier wavelength; (b) RF power at 10GHz as a function of DGD for different CD values for a 57-Gbit/s D8PSK system.

band FBG notch filter placed at 10 GHz away from the carrier in high-speed (19-GSym/s) transmission systems. The RF tone power at 10 GHz is used as a DGD monitoring signal, which is insensitive to the effects of CD. Compared with the monitoring techniques utilizing clock tone, the DGD monitoring range is increased to 50-ps and the bandwidth requirement of PD is reduced to 10 GHz.

### 3. System setup and experimental results

The experimental setup of CD-insensitive first-order PMD monitoring in a D8PSK system is shown in Fig. 2. Continuous wave (CW) tunable laser at the wavelength of 1550.02nm is launched into a transmission module. The symbol rate of the system is 19-Gsym/s. 38-Gbit/s DQPSK signal is generated by an in-phase/quadrature (IQ) modulator; and 57-Gbit/s D8PSK signal can be generated by phase modulating the DQPSK signal. The generated signal passes through several spans of dispersion compensation fiber (DCF), which provides CD from 0 to  $-330$ -ps/nm. Two polarization beam splitters (PBSs) and a tunable optical delay line are used as a first-order PMD emulator. At the monitoring branch, an FBG notch filter with bandwidth of 0.06nm and reflection of 15dB is placed at 10 GHz away from the carrier frequency such that the measured 10 GHz RF power is insensitive to CD. The filtered signal was received by a photodetector with a bandwidth of 10GHz. A RF spectrum analyzer is used to monitoring the 10 GHz RF tone powers. The RF spectrum analyzer can be replaced by a narrow band electrical filter and a power meter, which is cost effective. It is note that the narrowband FBG filter is only in the monitoring branch, and does not affect the received signal.

Figure 3(a) shows the optical spectrum (with resolution of 0.01nm) of a 57-Gbit/s D8PSK signal filtered by a narrow band FBG notch filter (with bandwidth of 0.06nm and reflection of 15dB). The optical component at 10 GHz away from the carrier was filtered out; therefore, the 10 GHz RF tone power is equivalent to that of SSB signal detected by PD. Figure 3(b) shows the 10 GHz RF tone power as a function of DGD in 57-Gbit/s D8PSK system. The power splitting ratio between the two principle-polarization-states is 0.5. Different CD values (0,  $-166$  and  $-330$ -ps/nm) were introduced by several spans of DCF. The intensity of 10 GHz RF tone reaches its minimum value when the DGD equals to 50-ps. This is due to the fact that the 10 GHz components of the two orthogonally-polarized signals have a phase shift of  $\pi$  and hence cancel out each other under DGD of 50-ps. The 10 GHz RF power varies as a function of DGD and the measurement range is increased to 50-ps, while it is only 26.3-ps if one of optical clocks is filtered out and 19 GHz RF tone is used as monitoring signal. It is observed that the 10 GHz RF tone power is not affect by CD value, which is consistent with the result calculated in part2. Moreover, our simulation results show the PMD monitoring results are almost not affected by CD value up to 1000 ps/nm.

The proposed scheme is also effective in DQPSK system. Figure 4(a) shows detected RF tone power at 10 GHz as a function of DGD in the 38-Gbit/s DQPSK system without FBG

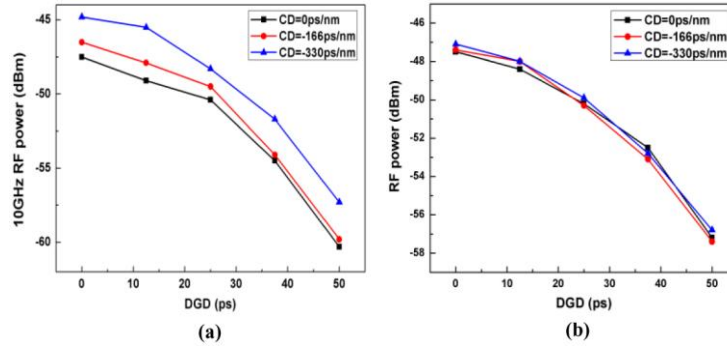


Fig. 4. RF power at 10GHz as a function of DGD for different CD values for a 38-Gbit/s DQPSK system (a) without filtering; (b) filtered by FBG notch filter placed at 10GHz away from carrier.

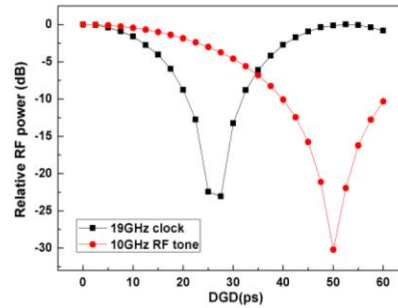


Fig. 5. Relative RF powers as a function of DGD for 38-Gbit/s DQPSK signal when 10 GHz RF tone and 19 GHz clock are monitoring signals.

filter. The signal was aligned at 45 degree respected to the PSPs of first-order PMD emulator. Several CD values (0, -166 and -330-ps/nm) were introduced. The CD induced RF power fluctuation is around 5dB. Figure 4(b) shows the results when the DQPSK signal is filtered by a narrow band FBG filter. The CD induced fluctuation is less than 1dB. It is noted that the FBG notch filter can be placed closer to the carrier, and the DGD measurement range will be increased further. However, the bandwidth of the FBG filter needs to be much narrower to avoid the filtering of carrier. Although the DGD measurement range is increased by using the lower frequency RF tone, the measurement accuracy will be decreased.

### 3. Further simulation results

Figure 5 shows the simulation results of relative 19 GHz RF clock and 10 GHz RF tone power as a function of DGD in 38-Gbit/s DQPSK system. The power splitting ratio between the two principle-polarization-states is 0.5. A FBG notch filter (with a rejection of 15 dB and 3 dB bandwidth of 0.06nm) was centered at clock and 10 GHz away from the carrier, respectively. The DGD measurement range is only 0~26.3-ps when the FBG filter is centered at one of optical clock and 19-GHz RF clock is used as monitoring signal, while the DGD measurement range is increased to 0~50-ps by using the 10 GHz RF tone as a monitoring signal. In the proposed method, the DGD measurement range is increased; however, the accuracy of DGD measurement decreases, especially in the small DGD region. There is a trade-off between accuracy and measurement range when RF tone is utilized as monitoring signal.

Figure 6(a) shows the effects of OSNR on the measurement results. It is observed that the dynamic range of RF power increases with OSNR. This is because the 10 GHz RF power reaches its minimum value when DGD equals to  $(NT + 1)/2$ . T is period time of 10 GHz RF tone and N is an integer. In these cases, the noise power is comparable to the RF power, and the measurement results are affected much by the noise. Therefore, the OSNR affects the

measurement results when RF power is small, where DGD is close to 50-ps. If the OSNR is smaller than 20 dB, the detected RF power has fluctuations and calibration is required.

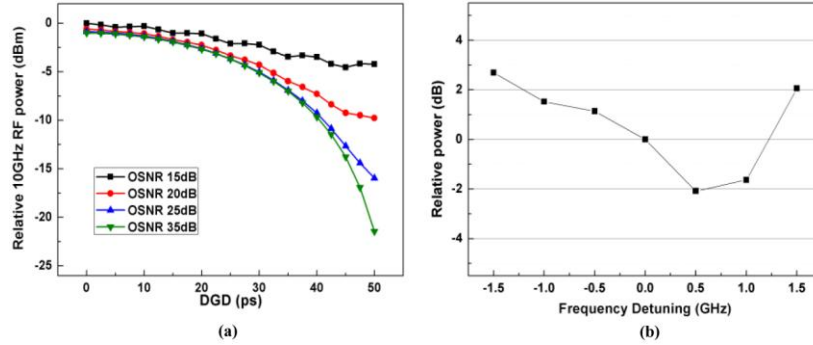


Fig. 6. (a) OSNR effects on the DGD measurement results; and (b) relative 10 GHz RF power as a function of DGD under FBG filter frequency detuning in 38-Gbit/s DQPSK system.

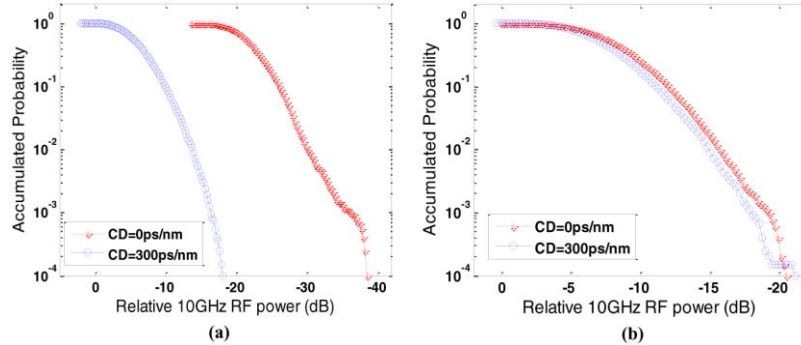


Fig. 7. Accumulated probability of relative 10GHz RF power for CD = 0 ps/nm and CD = 300 ps/nm (a) without filter; (b) with filter.

The center wavelength of FBG filter may shift from the original value under various environment effects, which may introduce RF power fluctuations and measurement errors. Figure 6(b) shows the effects of FBG frequency detuning on the 10GHz RF power in 38-Gbit/s DQPSK system. The 10GHz RF power change is less than 2dB when the FBG frequency detuning is smaller than 1GHz.

In order to investigate all-order PMD effect on the 10GHz RF power, a piece of nonlinear fiber includes both first-order and higher-order PMD was applied in the simulation. The average DGD of the fiber is 40-ps and the DQPSK signal was aligned at 45 degree respected to the PSP. Figure 7 shows the accumulated probability of relative 10GHz RF power under different CD values. 10000 samples were taken with CD at 0 and 300-ps/nm. Without FBG filter, the distribution of 10GHz RF power is affected by the CD value, shown in Fig. 7(a). If FBG filter is centered at one of sidebands, the CD effect on the distribution of 10GHz RF power can be eliminated, shown in Fig. 7(b).

#### 4. Conclusion

A CD-insensitive first-order PMD monitoring technique using FBG filter is presented in 38-Gbit/s DQPSK and 57-Gbit/s D8PSK systems. It is experimentally shown that the DGD measurement results are not affected by CD and the measurement range is increased to 50-ps in systems with a symbol rate of 19-GSym/s. Besides, the technique uses low-bandwidth PD (10GHz) and is therefore an efficient and cost effective PMD monitoring method.

#### Acknowledgement

The authors with National University of Singapore would like to thank the supports of A\*STAR SERC PSF 092 101 0054. And the authors with Jinan University would like to thank the supports of Fundamental Research Fund for the Central Universities (21609605).